Новые аспекты в физике аккрецирующих чёрных дыр

Гнедин Ю.Н., ГАО РАН

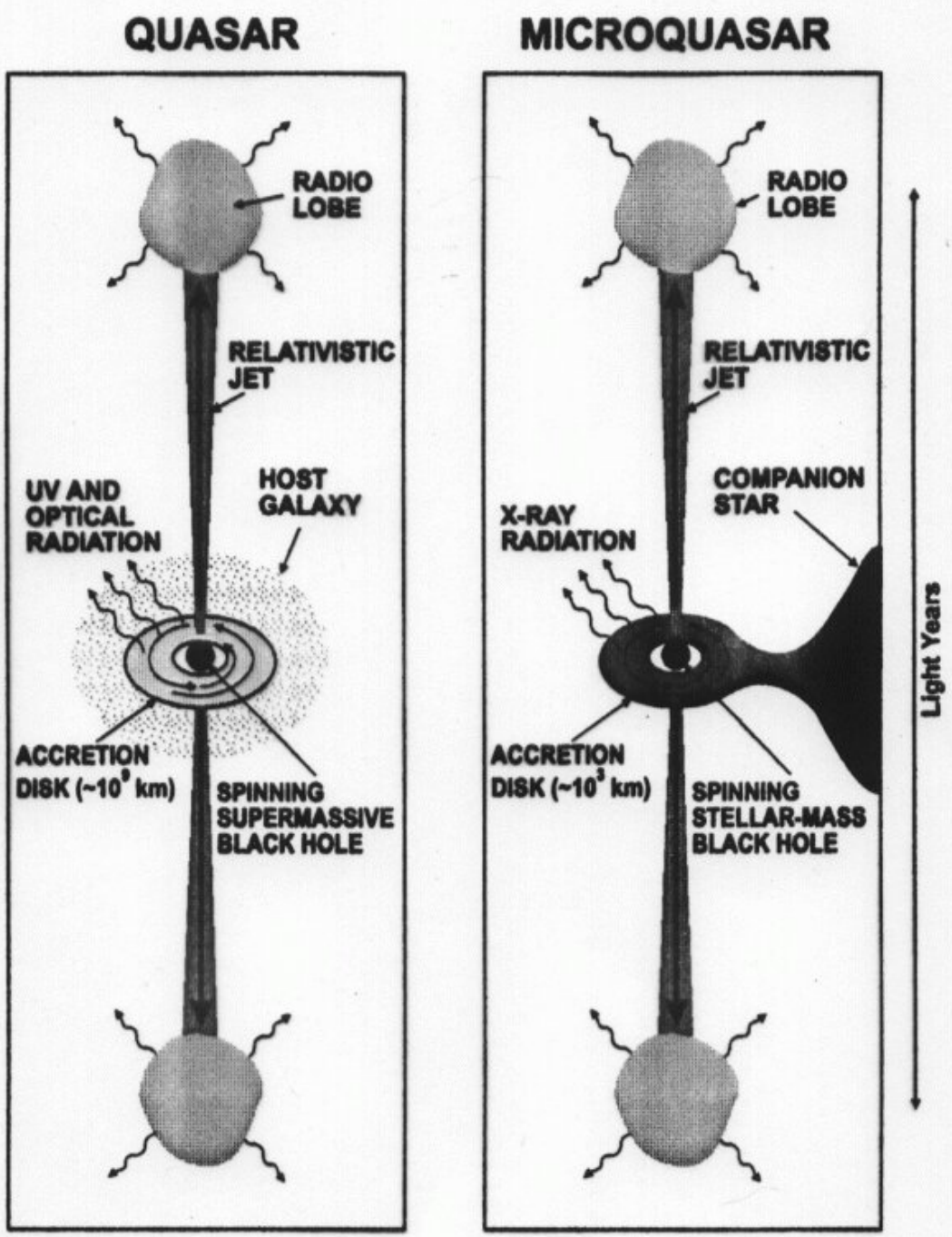

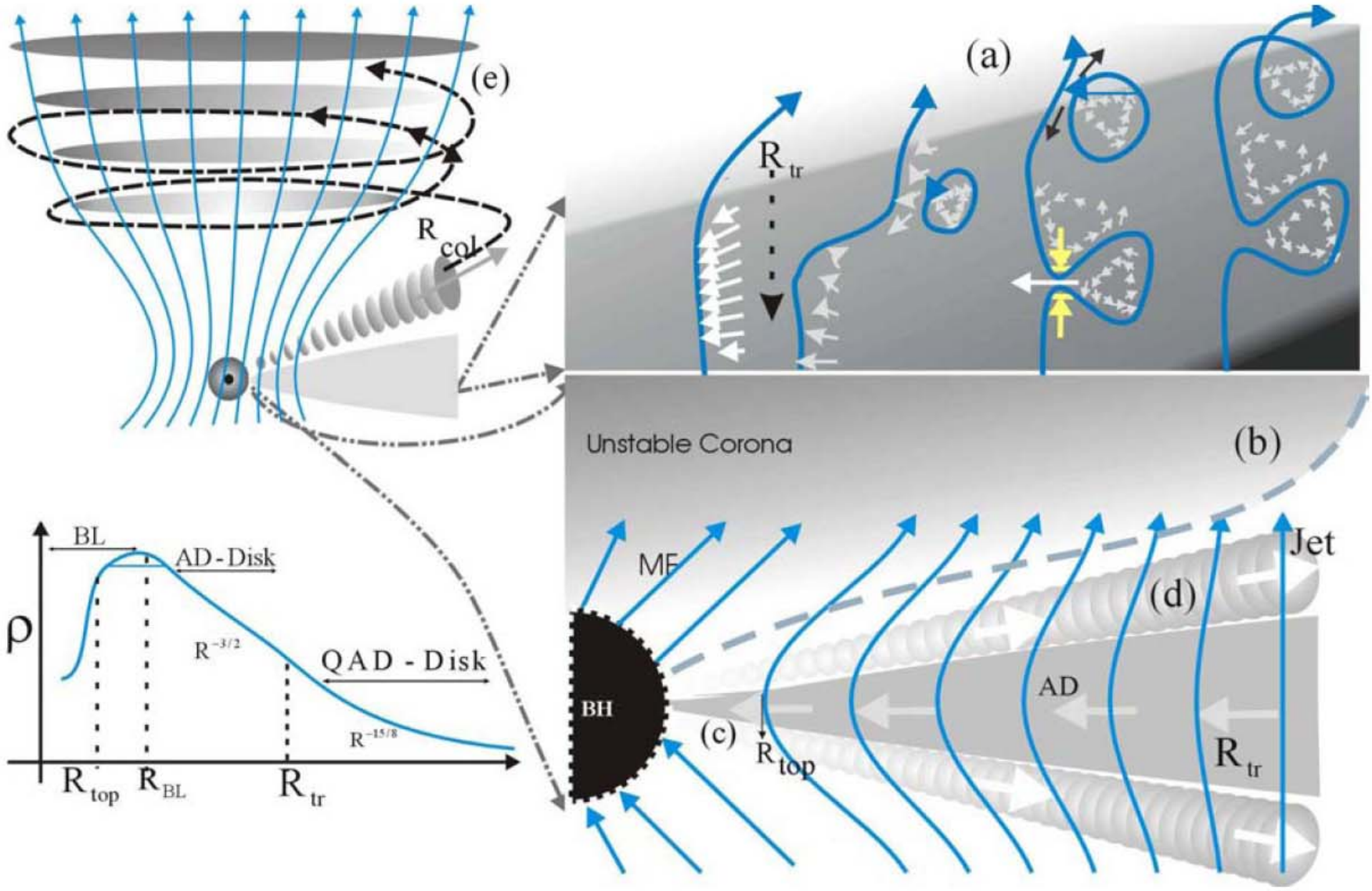
(e)
R col
(a)
R tr
Unstable Corona
(b)
Jet
MF
(d)
BH
(c)
AD
R top
R tr
ρ
BL
AD - Disk
R^-3/2
QAD - Disk
R^-15/8
R top
R BL
R tr

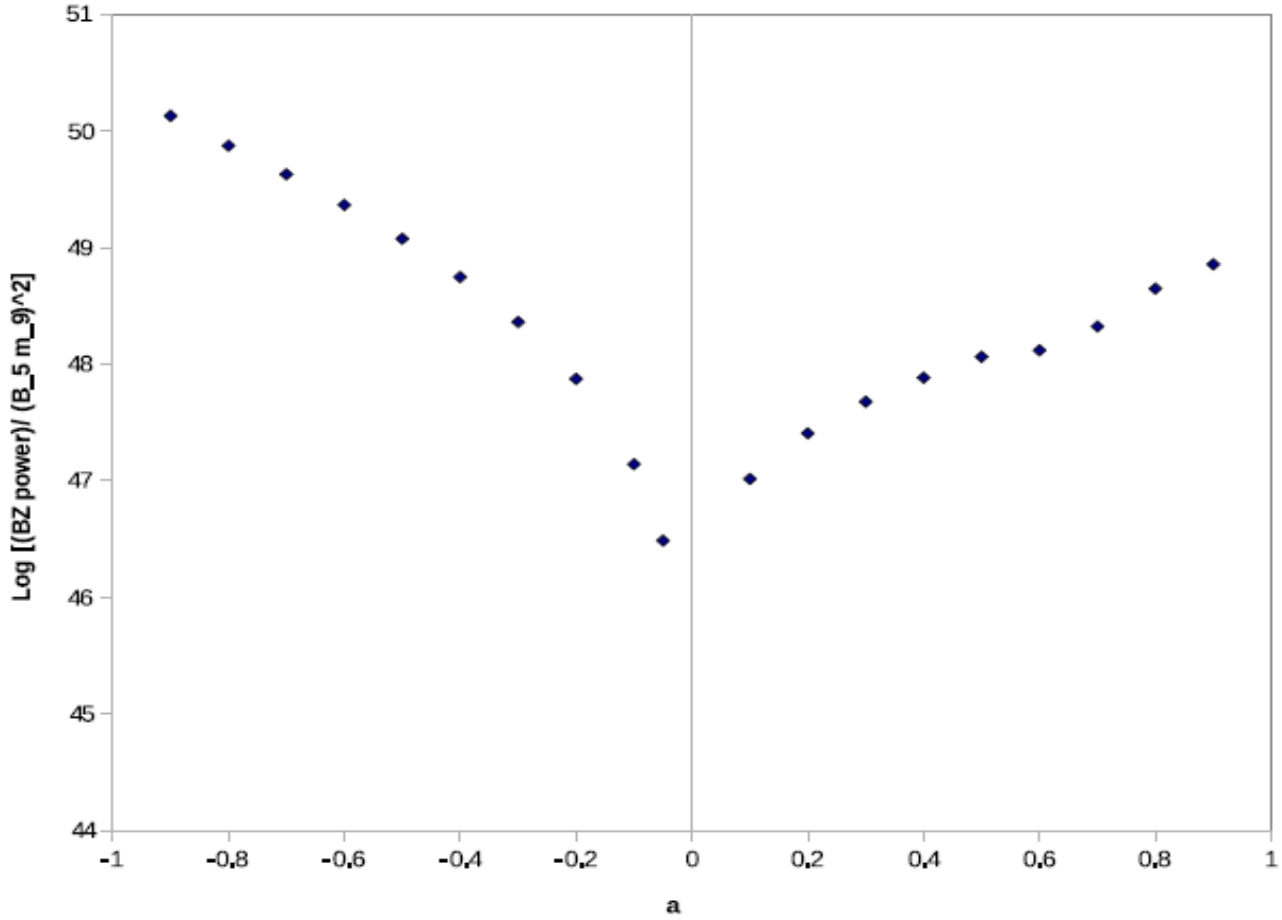

Figure 1. The BZ power vs spin accretion state (negative for retrograde and positive for prograde).

D. Garofalo, D.A. Evans, R.M. Sambruna, MNRAS, 2010

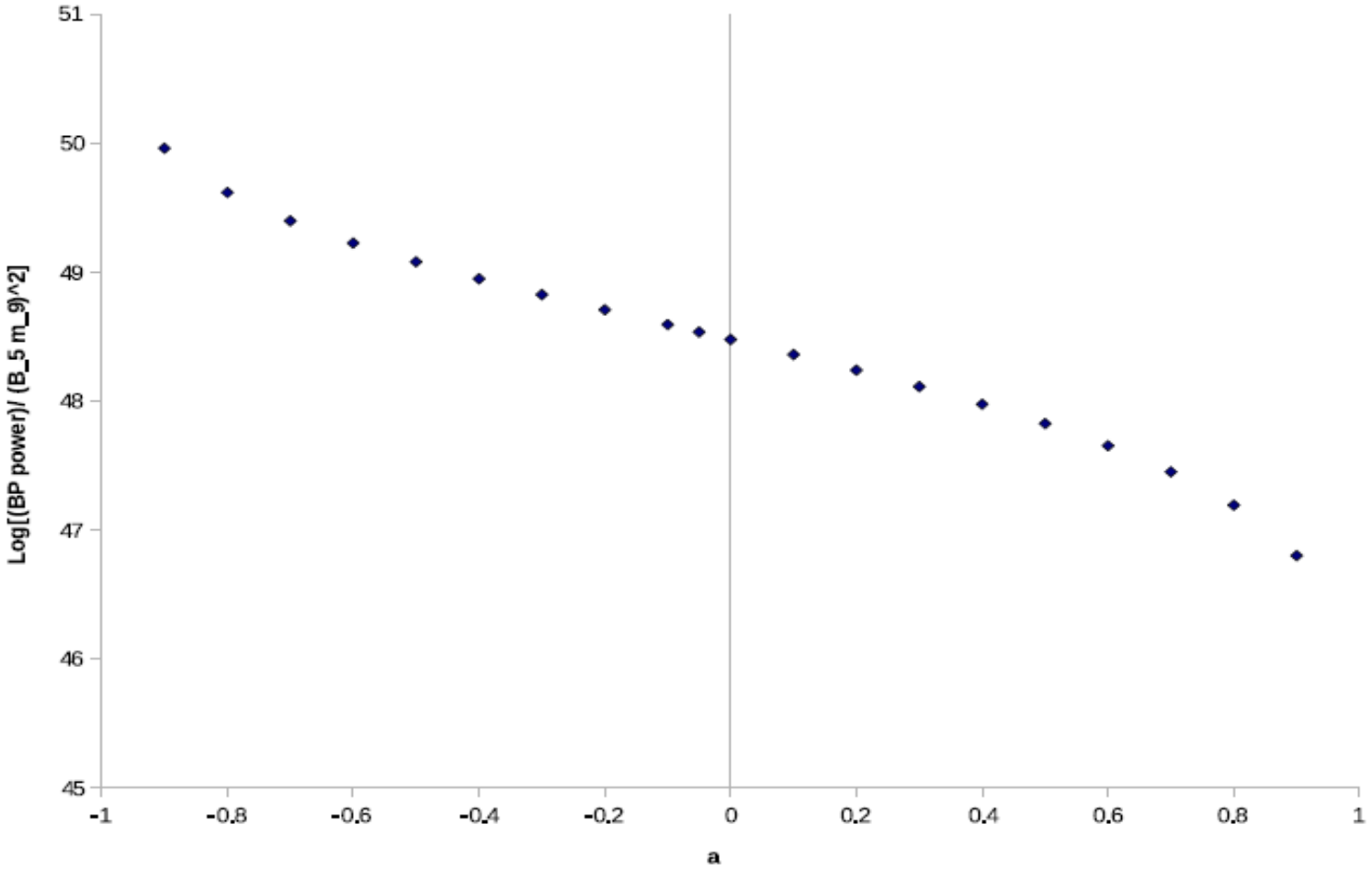

Figure 2. The BP power vs spin accretion state (negative for retrograde and positive for prograde).

D. Garofalo, D.A. Evans, R.M. Sambruna, MNRAS, 2010

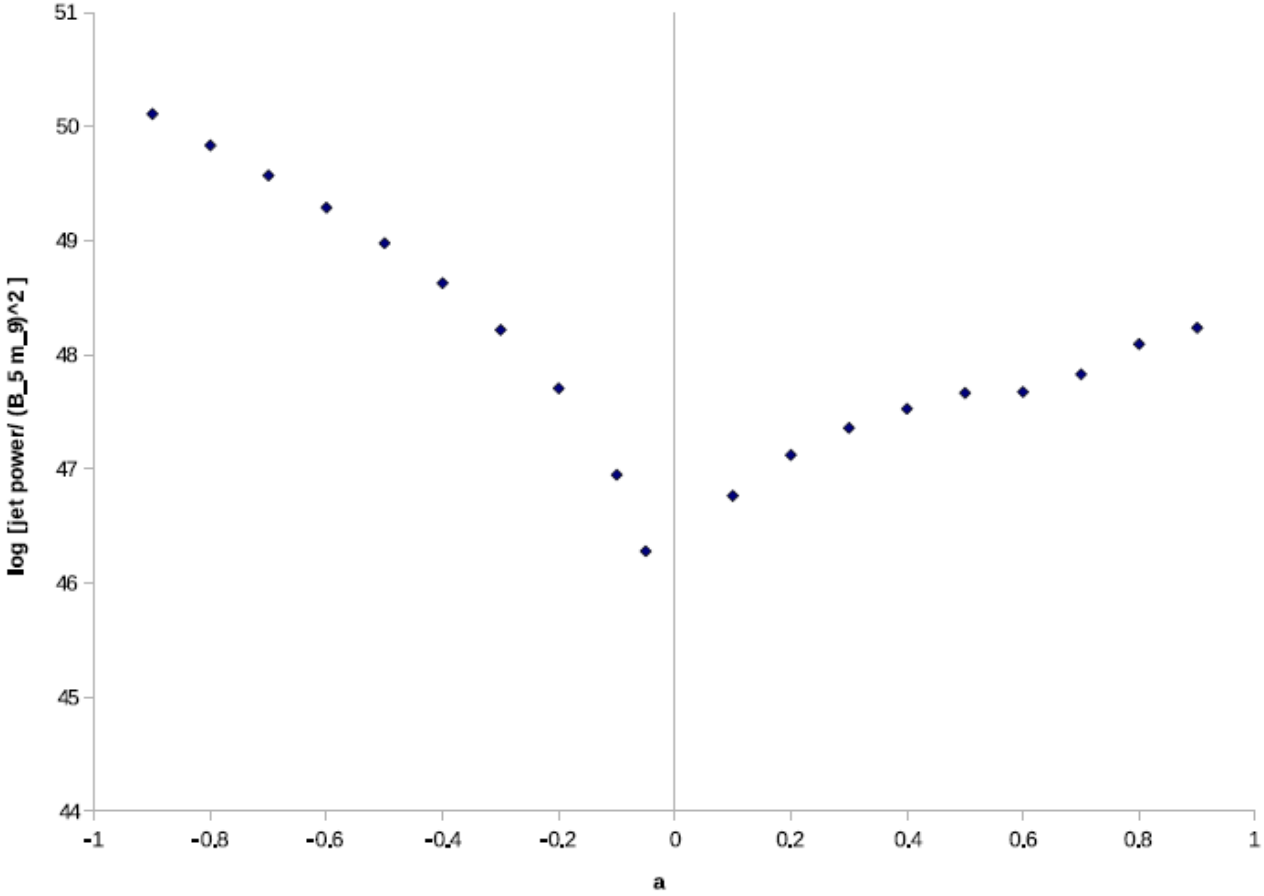

Figure 3. The overall jet power assuming BZ and BP operate in tandem via equation 20. B_5 is magnetic field in units of 10^5 Gauss and m is the ratio of black hole mass to 10^9 solar masses (i.e. for a 10^5 Gauss field, a 10^9 solar mass black hole, and a retrograde spin of -0.9, the power is slightly above 10^{50} erg/s). The value of δ is at a conservative estimate of about 2.5 but could be a magnitude or more higher. Numerical simulations of jets are needed to determine this value precisely. We emphasize that the discussion in section 4 implies that the above jet power dependence becomes irrelevant at high prograde spin in HERGs since the efficiency shifts from jets to disks.

D. Garofalo, D.A. Evans, R.M. Sambruna, MNRAS, 2010

A.Tchekhovskoy et al, ApJ, 699,1789, 2009

Две модели космических гамма-всплесков:

Magnetar: $$L_j = 2\times10^{47}\left(erg/s\right)\left(\frac{1ms}{p}\right)^2\left(\frac{B}{10^{15}G}\right)^2\left(\frac{R}{10km}\right)^2\left(\frac{\Theta}{10^0}\right)^4$$

Black Hole: $$L_j = 5\times10^{48}a^2\left(\frac{B_H}{10^{16}G}\right)^2\left(\frac{M_{BH}}{3M_\Theta}\right)^2\left(\frac{\Theta_k}{10^0}\right)^4 erg/s$$

Наш расчёт: BH with $a<0$ (retrograde rotation)

$$B_H = 10^{12.5}G,\quad a=-0.9$$

$$M_{BH} = 30M_\odot$$

Магнитное поле системы Cyg X-1

Нами получено *B* ~ 100 Гс в фотосфере звезды.
Фазовая зависимость более сложная, чем в случае модели дипольного поля, наклоненного к оси вращения системы. Похоже на квадруполь.
При фазе 0.5 (рентгеновский источник впереди) мы смотрим примерно на один из магнитных полюсов, а при фазе 0.0 – на другой.

Газовые потоки переносят поле к аккреционной структуре, на внешнем краю которой газ уплотняется. Из наших данных следует, что при этом *B* возрастает не более, чем в 6 - 10 раз:
***B* ~ *600 Гс* на расстоянии 6*10^11см = 2*10^5 Rg.**

Согласно стандартной модели замагниченного аккреционного диска Шакуры и Сюняева (1973):

$$B(R) = B(R_g)\left(\frac{R_g}{R}\right)^{5/4}$$

→на 3 *Rg* *B* ~ *10^9* Гс.
Если учесть, что внутри ~10--20 *Rg*, видимо, преобладает лучистое давление, то *B(3 Rg) ~ (2—3) 10^8 Гс*.

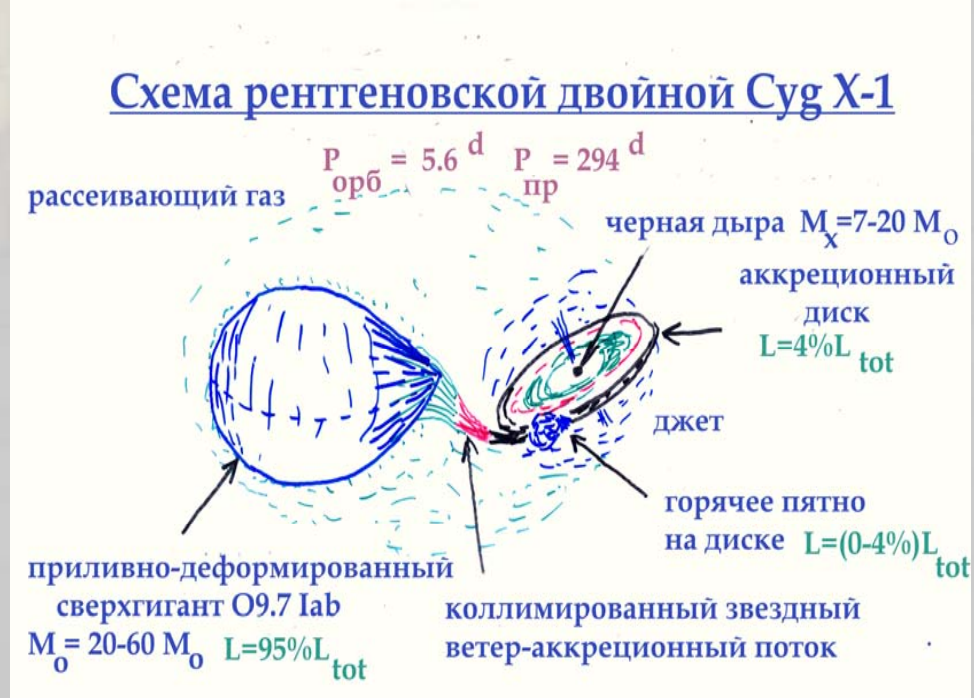

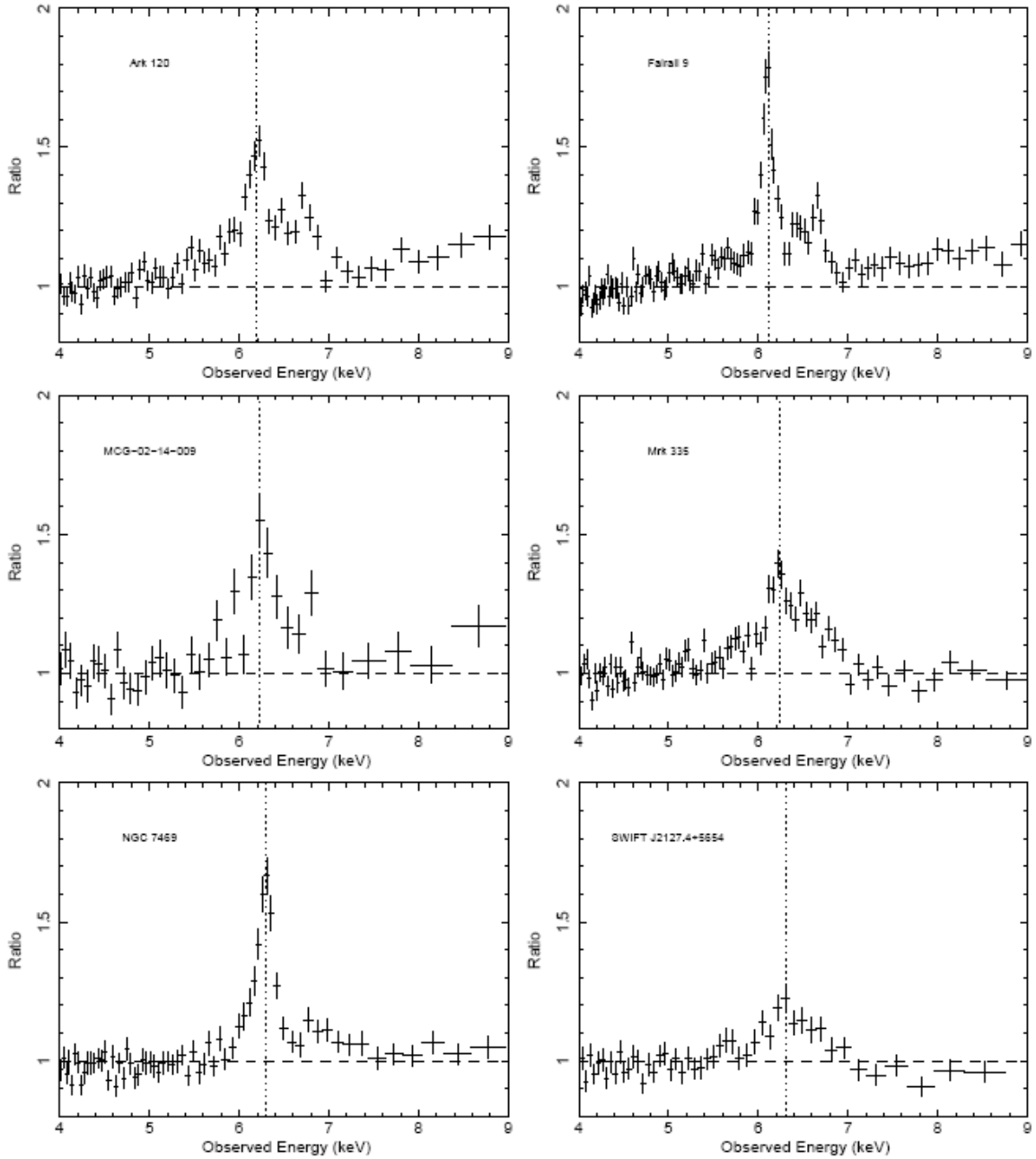

Figure 3. The 4–9 keV residuals after modelling of the continuum with a powerlaw, COMPTT to model the soft excess and Galactic photoelectric absorption. The dashed vertical line represents 6.4 keV in the rest frame.

Table 8. Fit parameters from Model E to *Suzaku* XIS, HXD and BAT data from *Swift*. (A) represents the unblurred REFLIONX and (B) represents the blurred REFLIONX. The ionization parameter ξ is given in units erg cm s^{-1}. [a] POWERLAW normalization given in units (10^{-2} ph keV^{-1} cm^{-2} s^{-1}). [b] REFLIONX normalization in units 10^{-5}. * denotes a parameter frozen at the best-fitting value from Model D. In some cases the spin parameter a could not be constrained, denoted by – .

	Ark 120	Fairall 9	MCG-02-14-009	Mrk 335	NGC 7469	SWIFT J2127.4+5654
Soft Excess	✓	✓	X	✓	✓	X
Γ	$2.12^{+0.01}_{-0.02}$	$2.01^{+0.01}_{-0.01}$	$1.90^{+0.03}_{-0.03}$	$2.15^{+0.01}_{-0.02}$	$1.80^{+0.01}_{-0.01}$	$2.20^{+0.05}_{-0.05}$
Norm [a]	$1.13^{+0.02}_{-0.02}$	$0.78^{+0.02}_{-0.02}$	$0.12^{+0.05}_{-0.03}$	$0.57^{+0.02}_{-0.02}$	$0.55^{+0.05}_{-0.07}$	$1.65^{+0.05}_{-0.08}$
			Kerrconv			
q	$4.1^{+0.8}_{-0.8}$	> 6.15	< 3.5	$6.6^{+2.0}_{-1.0}$	> 3.0	$2.2^{+0.6}_{-0.4}$
a	> 0.97	$0.98^{+0.01}_{-0.01}$	< 0.96	$0.87^{+0.05}_{-0.06}$	< 0.97	–
i°	48^{+3}_{-6}	70^{+5}_{-2}	40^{+11}_{-14}	53^{+6}_{-6}	70^{+4}_{-3}	43^{+18}_{-7}
Fe/Solar (A)	1.4*	1.9*	0.4*	$2.0^{+0.8}_{-0.4}$	1.6*	> 0.2
ξ (A)	< 13	< 11	< 543	< 11	< 11	< 26
Norm (A) [b]	$1.31^{+0.14}_{-0.15}$	$1.13^{+0.08}_{-0.19}$	$0.10^{+0.17}_{-0.10}$	$0.47^{+0.05}_{-0.10}$	$1.13^{+0.11}_{-0.21}$	$0.67^{+0.60}_{-0.60}$
Fe/Solar (B)	$1.5^{+0.3}_{-0.3}$	$0.8^{+0.2}_{-0.3}$	> 1.1	$1.0^{+0.1}_{-0.1}$	< 0.4	$1.0^{+0.8}_{-0.3}$
ξ (B)	56^{+12}_{-3}	24^{+17}_{-9}	< 14	207^{+5}_{-5}	< 24	< 14
Norm (B) [b]	$0.38^{+0.21}_{-0.13}$	$0.24^{+0.04}_{-0.03}$	$0.27^{+0.19}_{-0.20}$	$0.06^{+0.01}_{-0.01}$	$0.30^{+0.36}_{-0.12}$	$3.68^{+1.50}_{-1.99}$
FeXXV Line (keV)	$6.65^{+0.05}_{-0.07}$	$6.74^{+0.04}_{-0.04}$	–	$6.67^{+0.03}_{-0.03}$	–	–
EW (eV)	17^{+7}_{-7}	16^{+6}_{-6}	–	34^{+8}_{-8}	–	–
Flux (10^{-5} ph cm^{-2} s^{-1})	$0.62^{+0.26}_{-0.27}$	$0.44^{+0.17}_{-0.17}$	–	$0.55^{-0.13}_{-0.13}$	–	–
$\Delta\chi^2$	8	10	–	10	–	–
FeXXVI Line (keV)	$6.95^{+0.03}_{-0.03}$	$6.88^{+0.02}_{-0.03}$	$6.95^{+0.06}_{-0.07}$	$6.97^{+0.07}_{-0.12}$	–	–
EW (eV)	29^{+9}_{-9}	27^{+7}_{-7}	34^{+23}_{-23}	16^{+9}_{-8}	–	–
Flux (10^{-5} ph cm^{-2} s^{-1})	$0.85^{+0.27}_{-0.27}$	$0.63^{+0.17}_{-0.17}$	$0.14^{+0.10}_{-0.10}$	$0.23^{+0.13}_{-0.12}$	–	–
$\Delta\chi^2$	16	25	4	10	–	–
BAT const	$1.11^{+0.11}_{-0.11}$	$0.87^{+0.10}_{-0.10}$	–	$1.06^{+0.23}_{-0.23}$	$0.93^{+0.08}_{-0.08}$	$0.68^{+0.10}_{-0.09}$
χ^2_ν	770.2/647	879.6/832	612.0/538	811.6/722	835.4/808	830.4/865

Source	Mass ($M_\odot$)	Spin estimate: Disc	Spin estimate: Reflection	Refs
M33 X-7	15.6 ± 1.5	0.77 ± 0.05		1,6,7,17
LMC X-1	10.9 ± 1.4	$0.90^{+0.04}_{-0.09}$		1,7,18
LMC X-3	11.6 ± 2.1	< 0.8		4,7, 19
		-0.03		13
GS 2000+25	7.2 ± 1.7	0.03		1,13
GS 1124-68	6.0 ± 1.5	-0.04		1,13
4U 1543-47	9.4 ± 1.0	0.7–0.85	0.3 ± 0.1	1,2,3,7,8
GRO J1655-40	6.30 ± 0.27	0.65–0.8	0.98 ± 0.01	1,2,3,7,9
		0.93		13
GRS 1915+105	14 ± 4	0.98–1.0		1,2,5,7
		0–0.15		10
		~ 0.7		11
		0.998		13
XTE J1550-564	9.7–11.6	< 0.8	0.76 ± 0.01	1,4,7
XTE J1650-500	5 ± 2		0.79 ± 0.01	1,7
GX 339-4	≥ 6		0.94 ± 0.02	1,7
SAX J1711.6-3808			$0.6^{+0.2}_{-0.4}$	7
XTE J1908+094			0.75 ± 0.09	7
Cygnus X-1	10 ± 5		0.05 ± 0.01	1,7
4U 1957+11	3–16	0.8–1.0		1,12
A 0620-00	6.6 ± 0.3	$0.12^{+0.18}_{-0.20}$		21
MCG 6-30-15	$(4.5 \pm 2) \times 10^6$		$0.989^{+}0.009_{-0.002}$	14
SWIFT J2127.4+5654	$\sim 10^7$		0.6 ± 0.2	15
Fairall 9	$(2.6 \pm 0.6) \times 10^8$		0.60 ± 0.07	16
1H 0707-495	$\sim 10^7$		≥ 0.98	20

Table 1. A compilation of published spin (and mass) measurements for black holes in both X-ray binary systems and AGN, based on disc and reflection/line measurements. All of these measurements, except those of Zhang et al. (1997; see text for discussion) and the two upper limits, are presented in Fig 1. Ref 1 = Remillard & McClintock (2006) and McClintock & Remillard (2009), Ref 2 = McClintock, Narayan & Shafee (2007), Ref 3 = Shafee et al. (2006), Ref 4 = Davis, Done & Blaes (2006), Ref 5 = McClintock et al. (2006), Ref 6 = Liu et al. (2008), Ref 7 = Miller et al. (2009), Ref 8 = Gallo, Fender & Pooley (2003), Ref 9 = fender, homan & belloni and references therein, Ref 10 = Kato (2004), Ref 11 = Middleton et al. (2006), Ref 12 = Nowak et al. (2008), Ref 13 = Zhang et al. (1997), Ref 14 = Brenneman & Reynolds (2006), Ref 15 = Miniutti et al. (2009), Ref 16 = Schmoll et al. (2009, Ref 17 = Orosz et al. (2007), Ref 18 = Orosz et al. (2009), Ref 19 = Val-Baker, Norton & Negueruela (2007), Ref 20 = Fabian et al. (2009), Ref 21 = Gou et al. 2010 and references therein.

R. P. Fender, E. Gallo, D. Russell, MNRAS, 2010

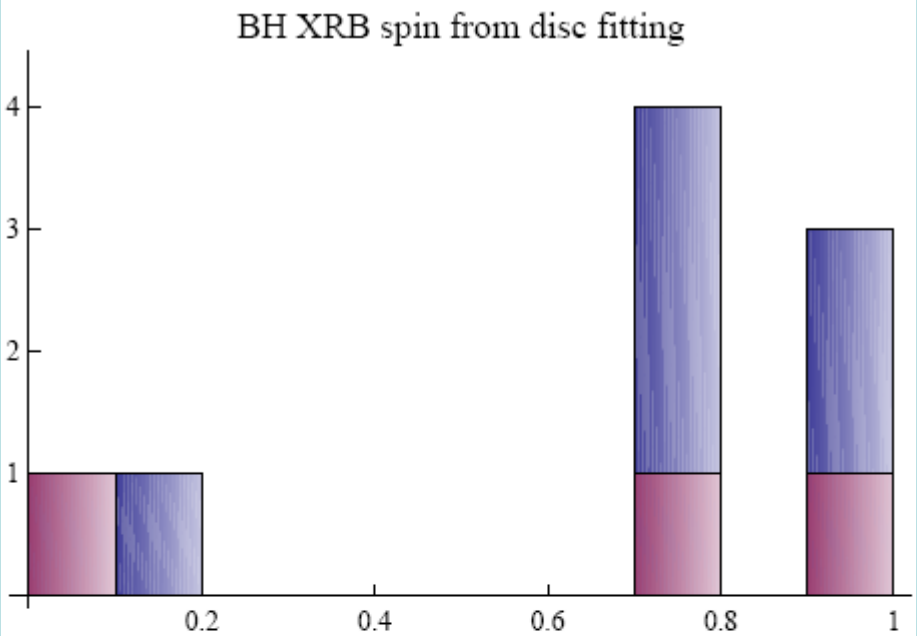
BH XRB spin from disc fitting
4
3
2
1
0.2
0.4
0.6
0.8
1

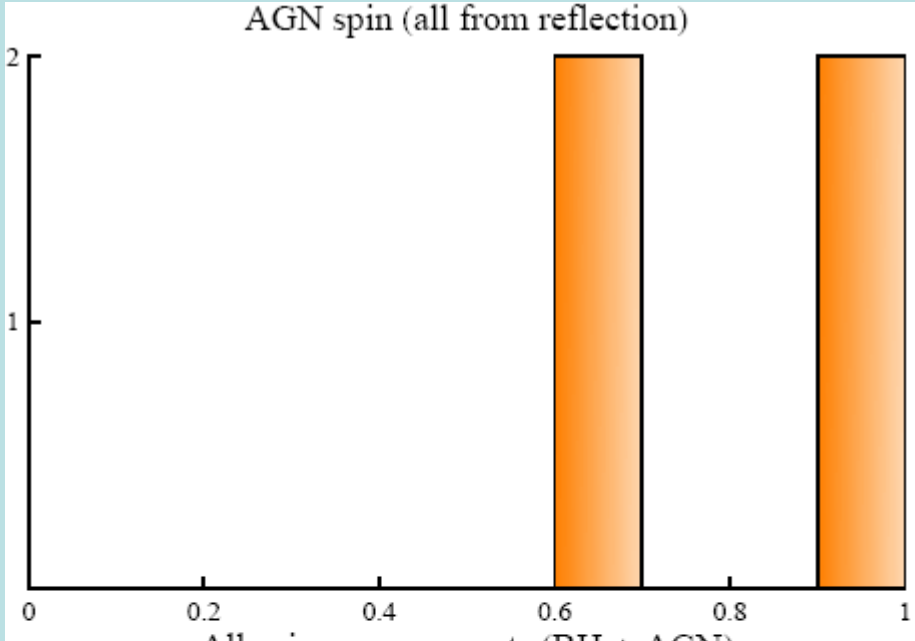
AGN spin (all from reflection)
2
1
0
0.2
0.4
0.6
0.8
1

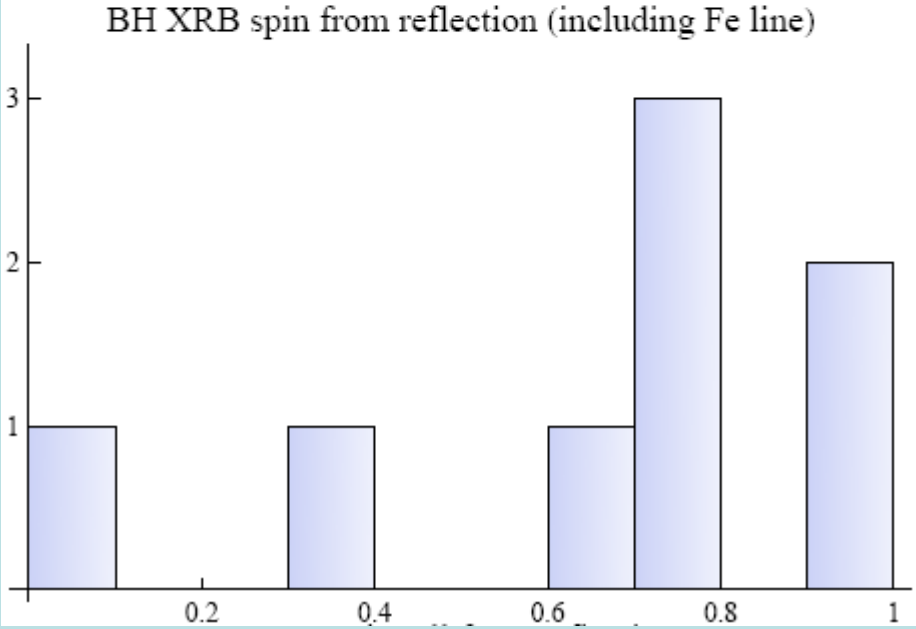
BH XRB spin from reflection (including Fe line)
3
2
1
0.2
0.4
0.6
0.8
1

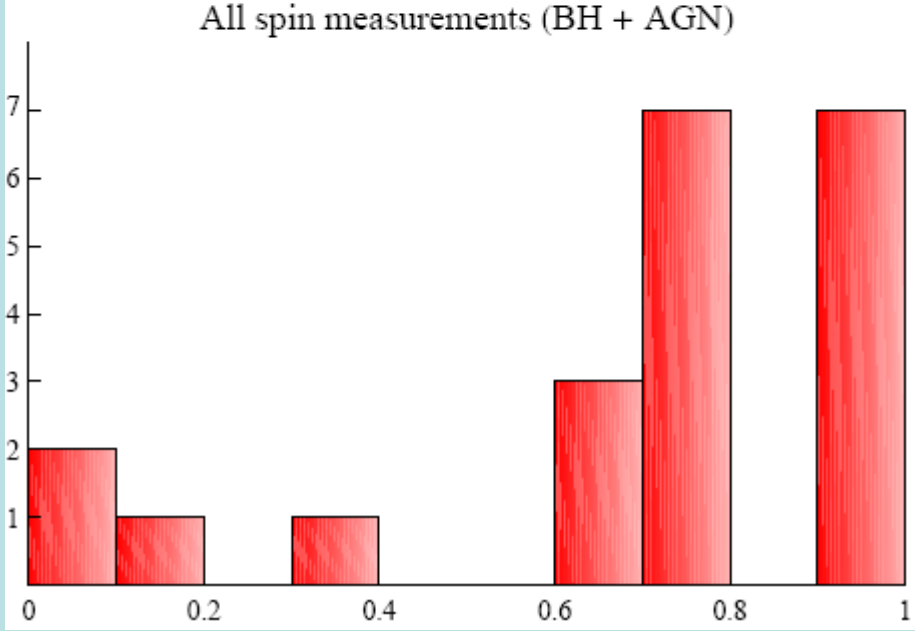
All spin measurements (BH + AGN)
7
6
5
4
3
2
1
0
0.2
0.4
0.6
0.8
1

Table 5. Central BH Masses (10^9 $M_\odot$)

Quasar (SDSS)	L_{Bol}[a]	L_{Bol}/L_{Edd}[b]	M_{BH}(C IV)	M_{BH}(Mg II)	M'_{BH}(Mg II)[c]
J0836+0054	47.72	0.44	9.3±1.6	...	...
J1030+0524	47.37	0.50	3.6±0.9	1.0±0.2	2.1±0.4
J1044−0125	47.63	0.31	10.5±1.6	...	...
J1306+0356	47.40	0.61	3.2±0.6	1.1±0.1	2.2±0.3
J1411+1217	47.20	0.94	1.3±0.3	0.6±0.1	0.9±0.2
J1623+3112	47.33	1.11	...	1.5±0.3	...

[a]Bolometric luminosity in log[erg s^{-1}] from Jiang et al. (2006).

[b]L_{Edd} is derived from M_{BH}(C IV) except for SDSS J1623+3112, whose L_{Edd} is derived from M_{BH}(Mg II).

[c]M'_{BH} is estimated from the new relation by Vestergaard et al. (in preparation).

Магнитные поля AGN (Equipartition)

R.-Y. Ma, F. Yuan, arXiv:0706.0124.

$$B_H = k\sqrt{2L_{bol}/\varepsilon c}/R_H, \quad k \approx 1$$

$$L_{bol} = \varepsilon \dot{M} c^2, \quad R_H = \frac{GM}{c^2}\left(1+\sqrt{1-\left(\frac{a}{M}\right)^2}\right)$$

a/M	ϵ_M	Spin Equilibrium?	Characterization
0.0	0.057	no	standard thin disk; nonspinning BH
0.95	0.19	yes	turbulent MHD disk
0.998	0.32	yes	standard thin disk; photon recapture
1.0	0.42	yes	standard thin disk; max spin BH

$$B_{Ed} = 6.2\times10^8\left(\frac{M_\odot}{M_{BH}}\right)^{1/2}\left(\frac{\eta}{\varepsilon}\right)^{1/2}\frac{1}{1+\sqrt{1-\left(\frac{a}{M}\right)^2}}, \quad \eta = \frac{L_{bol}}{L_{Ed}}$$

Магнитные поля квазаров в эпоху вторичной ионизации.

Квазар	**z**	**L_{bol}/L_{Ed}**	**a/M = 0, ε = 0.057**	**a/M = 0.95, ε = 0.19**	**a/M = 0.998, ε = 0.32**	**a/M = 1.0, ε = 0.42**
J0836+0054	5.810	0.44	9.0×10^3 G	7.5×10^3 G	7.15×10^3 G	6.6×10^3 G
J1030+0524	6.309	0.50	1.5×10^4 G	1.22×10^4 G	1.16×10^4 G	1.0×10^4 G
J1044-0125	5.778	0.31	7.1×10^3 G	6.0×10^3 G	5.7×10^3 G	5.3×10^3 G
J1306+0356	6.016	0.61	1.8×10^4 G	1.5×10^4 G	1.43×10^4 G	1.4×10^4 G
J1411+1217	5.927	0.94	3.5×10^4 G	2.93×10^4 G	2.8×10^4 G	2.7×10^4 G
J1623+312	6.247	1.11	3.5×10^4 G	2.93×10^4 G	2.8×10^4 G	2.7×10^4 G

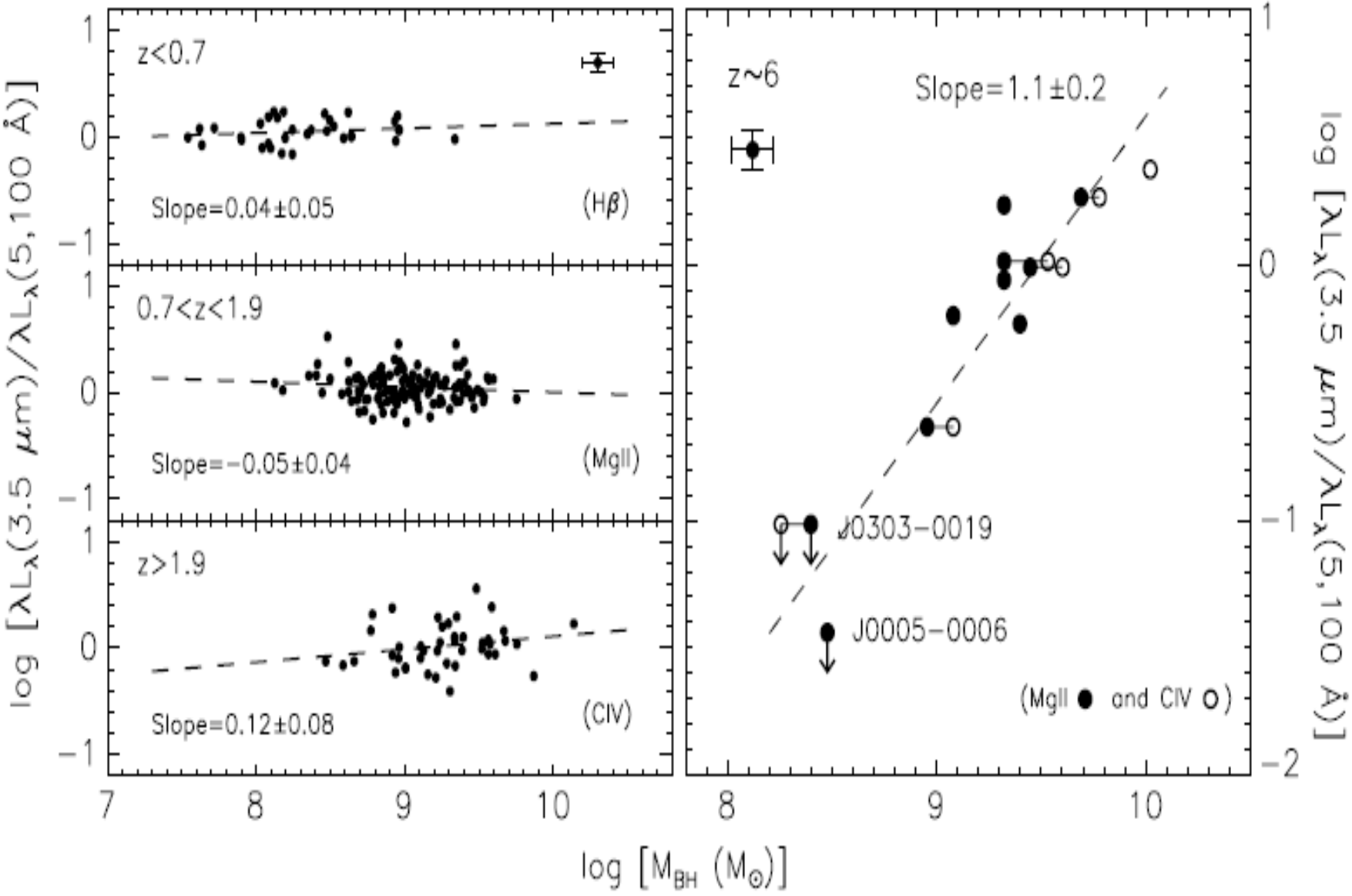

Linhua Jiang, Xiaohui Fan, et al. arXiv.1003.3432

Проблема зарождения массивных черных дыр в эпоху вторичной ионизации Вселенной.

t_o **- observation,** t_S **- seed,** $M_{BH}\left(t_o\right)=M_{BH}\left(t_S\right)\exp\left[\eta\frac{1-\varepsilon}{\varepsilon}\frac{t_o-t_S}{\tau}\right];\ \eta=\frac{L}{L_{Edd}},$

$$\tau=\frac{\dot{M}c^2}{L_{Edd}}=0.45\times10^9\ \textbf{yrs – Salpeter Time (M/ Begelman)}$$

$$B\left(seed\right)=B_H\left(t_o\right)\exp\left[\eta\frac{1-\varepsilon}{\varepsilon}\frac{\left(t_o-t_S\right)}{2\tau}\right]$$

Two most popular accretion models: $M_{seed}\le10^2M_\odot,\ M_{seed}\ge10^3M_\odot.$

Стандартная космология.

$$\frac{a}{M}=0:M_{seed}\sim10^2M_\odot,z_s=20\div30;\ \frac{a}{M}=0.95:M_{seed}\sim10^3M_\odot,z_s=20\div30;$$

$$\frac{a}{M}=1.0:M_{seed}\sim10^5M_\odot,z_s>20;$$

Керровские черные дыры образуются путем слияния (merging), а не аккреции?!

Кинетическая энергия джета квазаров в эпоху вторичной ионизации

$$a_* = 0.998 \qquad \varepsilon = 0.32$$

J0836+0054 $M_{BH} = 9.3\times10^9 M_\odot$ $z = 5.810$

$L_j = 3.9\times10^{49} erg/s$ $L_{Edd} = 2.6\times10^{47} erg/s$

J1030+0524 $M_{BH} = 3.6\times10^9 M_\odot$ $z = 6.309$

$L_j = 1.5\times10^{49} erg/s$

J1044-0125 $M_{BH} = 10.5\times10^9 M_\odot$ $z = 5.778$

$L_j = 3.16\times10^{49} erg/s$ $L_{Edd} = 1.4\times10^{48} erg/s$

$$L_j = 5.8\times10^{43}\left(\frac{L_R}{10^{40}}\right)^{0.7}$$ - K.W.Cavagnolo et al., arXiv 1006.5699, 29 Jun 2010

$$\log\left(\frac{L_j}{L_{Ed}}\right) = (0.49\pm0.07)\log\left(\frac{L_{bol}}{L_{Ed}}\right) - (0.78\pm0.36)$$

$L_R = L(5GHz)$ Merloni and Heintz, 2007, MNRAS, 381

Willott et al., 1999, MNRAS, 309, 1017

$$L_j = 1.4\times10^{37}\left(\frac{L_{1.4GHz}}{10^{25}W/Hz}\right)^{0.85} W, \quad L_{1.4} > 10^{25}W/Hz$$

$$L_{1.4} < 10^{25}W/Hz, \quad L_j = 1.2\times10^{37}\left(\frac{L_{1.4}}{10^{25}W/Hz}\right)^{0.4} W$$

Punsly (2005) astro-ph/0503267

$$L_j = 5.7\times10^{44}\left[(1+z)^{1-\alpha}\, y^2(z) F_{151}\right]^{\frac{6}{7}} erg/s: \quad F_{151} \equiv F_{151MHz}$$

$$y(z) = \int_0^z \frac{dx}{H(x)/H_0}$$

Table 2. New circular polarization measurements of quasars

Object	z	$p_{\rm lin}$ (%)	$\theta_{\rm lin}$ (°)	$p_{\rm circ}$ (%)
1120+019	1.465	1.95 ± 0.27	9 ± 4^{c}	−0.02 ± 0.05
1124−186	1.048	11.68 ± 0.36	37 ± 1^{g}	−0.04 ± 0.08
1127−145	1.187	1.30 ± 0.40 [w]	23 ± 10^{a}	−0.05 ± 0.05
1157+014	1.990	0.76 ± 0.18	39 ± 7^{f}	−0.10 ± 0.08
1205+146	1.640	0.83 ± 0.18	161 ± 6^{f}	−0.10 ± 0.09
1212+147	1.621	1.45 ± 0.30	24 ± 6^{c}	0.15 ± 0.09
1215−002⋆	0.420	23.94 ± 0.70	91 ± 1^{g}	−0.42 ± 0.40
1216−010	0.415	11.20 ± 0.17	100 ± 1^{g}	−0.01 ± 0.07
1222+228	2.058	0.92 ± 0.14	169 ± 4^{g}	0.01 ± 0.10
1244−255	0.633	8.40 ± 0.20 [w]	110 ± 1^{a}	−0.23 ± 0.20
1246−057	2.236	1.96 ± 0.18 [w]	149 ± 3^{e}	0.01 ± 0.03
1254+047	1.024	1.22 ± 0.15 [w]	165 ± 3^{b}	−0.02 ± 0.04
1256−229⋆	0.481	22.32 ± 0.15	157 ± 1^{g}	0.18 ± 0.04
1309−056	2.212	0.78 ± 0.28	179 ± 11^{c}	−0.08 ± 0.06
1331−011	1.867	1.88 ± 0.31	29 ± 5^{c}	−0.04 ± 0.06
1339−180	2.210	0.83 ± 0.15	20 ± 5^{g}	−0.01 ± 0.07
1416−129	0.129	1.63 ± 0.15 [w]	44 ± 3^{b}	0.05 ± 0.06
1429−008	2.084	1.00 ± 0.29	9 ± 9^{c}	0.02 ± 0.08
2121+050	1.878	10.70 ± 2.90 [w]	68 ± 6^{a}	0.02 ± 0.15
2128−123	0.501	1.90 ± 0.40 [w]	64 ± 6^{d}	−0.04 ± 0.03
2155−152	0.672	22.60 ± 1.10 [w]	7 ± 2^{a}	−0.35 ± 0.10

Notes: Linear and circular polarizations were measured in the V filter except a series of linear polarization data from the literature measured in white light and noted [w]; (⋆) 1215−002 is classified as a BL Lac by Collinge et al. 2005; Sbarufatti et al. 2005 re-determined the redshift of 1256−229 (z=0.481) and considered this object as a BL Lac. References for linear polarization: (a) Impey & Tapia 1990; (b) Berriman et al. 1990; (c) Hutsemékers et al. 1998; (d) Visvanathan & Wills 1998; (e) Schmidt & Hines 1999; (f) Lamy & Hutsemékers 2000; (g) Sluse et al. 2005.

D. Hutsemekers et al.

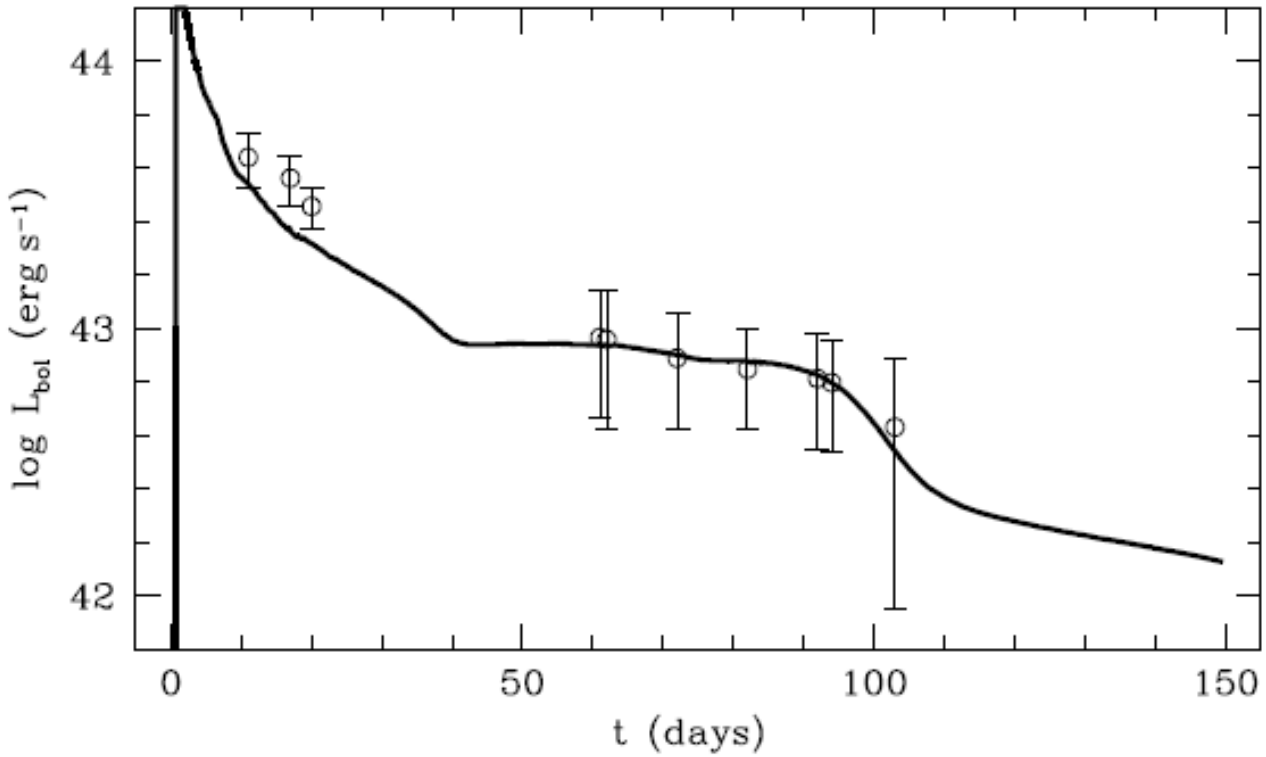

Fig. 2.— The calculated bolometric light curve of the optimal model (*solid line*) overplotted on the bolometric data of the black-body fit for SN 2009kf (*open circles*).

Table 1. FR II Quasars with Super Eddington Jets

Source	z	$\overline{Q}$ 10^{45}ergs/s	L_{bol} 10^{45}ergs/s	$\overline{R}$	freq (10^{15} Hz)	L_{bol}/L_{Edd}	$\overline{Q}_{Edd}$	ref
3C 216	0.670	15.1/14.1	≈ 0.12	≈ 120	0.71/1.16	$0.05-0.1$	$3.3-10$	1
3C 455	0.543	7.13/5.04	0.38	18.7/13.3	0.94	1.42	26.7/18.9	2
		7.13/5.04	0.38	18.7/13.3	0.94	0.07	1.33/0.94	3
3C 82	2.878	155.4/183.8	14.5	10.7/12.7	0.014	0.106	1.14/1.35	4
		155.4/183.8	25.0	6.22/7.35	1.67	0.245	1.52/1.80	4
3C 9	2.009	148.3/174	25.0	5.93/6.96	1.67	0.264	1.57/1.85	5
		148.3/174	38.8	3.82/4.49	0.0078	0.324	1.24/1.46	6
4C 25.21	2.686	59.3/59.7	11.6	5.11/5.15	1.14	0.198	1.02/1.02	5
PKS 1018-42	1.28	63.9/65.2	19.3	3.31/3.38	1.37	0.428	1.42/1.45	7
		63.9/65.2	14.7	4.35/4.45	1.37	0.326	1.42/1.45	7
4C 04.81	2.594	103.8/148	35.8	2.90/4.13	2.30	0.459	1.33/1.90	5
3C 196	0.871	73.5/87.0	31.6	2.33/2.76	1.53	3.04	7.10/8.41	8
		73.5/87.0	31.6	2.33/2.76	1.53	0.238	0.66/0.56	9
3C 14	1.469	52.38/51.68	32.6	1.61/1.59	1.00	0.604	1.05/1.03	10
3C 270.1	1.519	65.1/66.6	48.2	1.35/1.38	2.07	0.844	1.14/1.17	5

1. see Punsly (2007), 2. continuum and FWHM from Gelderman and Whittle (1994), M_{bh} from eqn (5), 3. M_{bh} from bulge luminosity estimate in eqn (8), 4. L_{bol} and FWHM raw data from Semenov et al. (2004), M_{bh} from eqn (6), 5. L_{bol} and FWHM from Barthel et al. (1990), M_{bh} from eqn (6), 6. continuum from Meisenheimer et al. (2001), FWHM from Barthel et al. (1990),M_{bh} from eqn(6), 7. Punsly and Tingay (2006), M_{bh} from eqn(7), 8. continuum and FWHM from Lawrence et al. (1996), M_{bh} from eqn (5), 9. continuum and FWHM from Lawrence et al. (1996), M_{bh} from eqn (7), 10. continuum and FWHM from Aars et al (2005), M_{bh} from eqn (7)